Physics Letters A 378 (2014) 3131–3135

Contents lists available at ScienceDirect

Physics Letters A

www.elsevier.com/locate/pla

Effective manipulation of Andreev bound states, zero mode Majorana fermion and Josephson current in a superconductor–normal–superconductor junction on the surface of a topological insulator

Kun-Hua Zhang [a], Zhen-Gang Zhu [a,b,*,1], Zheng-Chuan Wang [a], Qing-Rong Zheng [a,*], Gang Su [a,*]

[a] Theoretical Condensed Matter Physics and Computational Materials Physics Laboratory, School of Physics, University of Chinese Academy of Sciences, Beijing 100049, China

[b] School of Electronic, Electrical and Communication Engineering, University of Chinese Academy of Sciences, Beijing 100049, China

ARTICLE INFO

Article history:
Received 24 August 2014
Accepted 29 August 2014
Available online 6 September 2014
Communicated by V.M. Agranovich

Keywords:
Andreev bound states
Majorana fermion
Josephson current
Surface states
Topological insulator

ABSTRACT

We study the effective manipulation of the Andreev bound states (ABS), zero mode Majorana fermion and Josephson current (JC) in a superconductor–normal–superconductor junction on the surface of a topological insulator in unexplored regime of parameters. It is found that the energy of the ABS changes dramatically with the phase difference between both superconductors (SCs) in a certain range of the incident angle of quasiparticles. It is shown that the velocity of Majorana fermion and the JC can be effectively tuned in a wide range of the chemical potential in the normal region (μ_N) and the separation width (L) of the two SCs. In addition, we expose that the critical JC and its product with the normal resistance are, respectively, a quarter and the same to those in a graphene-based Josephson junction. The dependence of the critical JC on the chemical potential in the superconducting region is not monotonous: it increases (decreases) for small (large) μ_N.

1. Introduction

Topological insulators (TIs) are proposed as new quantum states of matter, which have a bulk band gap and gapless edge states or metallic surface states due to the time reversal symmetry and spin–orbit coupling [1–6]. The topologically protected metallic surface states in TIs have been observed by surface-sensitive experimental techniques, such as angle-resolved photoemission spectroscopy (ARPES) [7–9] and scanning tunneling microscopy (STM) [10,11]. Furthermore, a negligible contribution to transport from bulk carriers [12] and near 100% contribution from the surface states of TIs [13] have been identified in experiments. Recently, Fu and Kane [14] have proposed that a gapped surface state of a strong TI induced by the proximity effect of an s-wave superconductor resembles a spinless $p_x + ip_y$ superconductor. This $p_x + ip_y$ superconducting state was predicted to host Majorana fermion excitations, which are expected to have potential applications in quantum information [15]. The prediction by Fu and Kane spurred much interest on the superconductivity of topological surface states. The superconducting energy-gap induced by the proximity effect and supercurrent in a topological insulator Josephson junction (TIJJ) has been observed in experiments [16–23]. How to manipulate and detect the Majorana fermions were also addressed theoretically in the TIJJ and a superconductor–TI–magnet junction [14,24–26].

It is also interesting to address the Andreev bound states and the current–phase relation in the TIJJ system [27–32]. The Bogoliubov quasiparticle corresponding to the zero energy Andreev bound state is Majorana fermion in the TIJJ [14], when the phase difference between two superconductors is π in the TIJJ. Since the chemical potential μ of the surface states can be tuned by an external gate voltage or a chemical doping in experiments, the chemical potential μ_N in normal surface region (we mean the region of TI without covering a superconductor) and μ_S in superconducting region can be different in general. The current–phase relation of a Josephson junction has been studied under the condition of $\mu_S = 2\Delta$ and μ_N varying from 0 to 4Δ in Ref. [28], where Δ is the superconducting energy gap. A nearly flat Andreev bound state spectrum is concluded in the case of a fixed phase difference π, $\mu_N = \mu_S \sim 17\Delta$ and $L \sim \xi$ in Ref. [29], where L is the

* Corresponding authors.
E-mail addresses: zgzhu@ucas.ac.cn (Z.-G. Zhu), qrzheng@ucas.ac.cn (Q.-R. Zheng), gsu@ucas.ac.cn (G. Su).
[1] Correspondence to: Theoretical Condensed Matter Physics and Computational Materials Physics Laboratory, School of Physics, University of Chinese Academy of Sciences, Beijing 100049, China.

http://dx.doi.org/10.1016/j.physleta.2014.08.033
0375-9601/

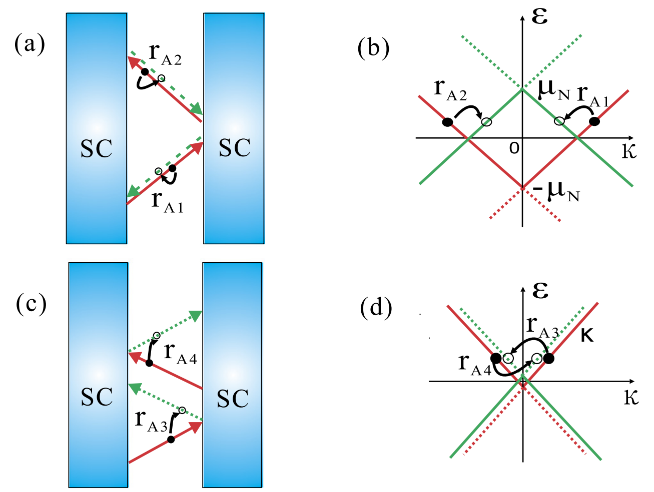

Fig. 1. (Color online.) Schematic top-view of layout of a superconductor–normal–superconductor junction on the surface of a topological insulator shown in (a) and (c), where SC indicates the s-wave superconductor. r_{Ai}, $i = 1, 2, 3, 4$ correspond the processes shown in (b) and (d). (a) and (b) show the Andreev retroreflection for $\varepsilon < \mu_N$, (c) and (d) correspond to the specular Andreev reflection $\varepsilon > \mu_N$, (b) and (d) depict the excitation spectrum of normal topological surface states, where the red (green) lines indicate electron (hole) excitations, and the solid (dashed) lines indicate conduction (valence) bands.

junction width and ξ is the superconducting coherence length. Since $\mu_S \gg \Delta$ is the most common experimental situation in ordinary superconductor [26,30,33], it is more reasonable to set a large μ_S, which is very far away from the Dirac point. This case was studied in Ref. [30] under an assumption of very large fixed μ_N (accounted from the Dirac point), and the 4π periodic Andreev bound states was anticipated. Moreover, the anomalous supercurrent in the TIJJ was studied in the presence of an applied magnetic field [32].

In this paper, we study the Andreev bound states and Josephson current in a superconductor–normal–superconductor (SNS) junction on the surface of a topological insulator, under the conditions of $\mu_S \gg \Delta$, and L is shorter than ξ, where μ_N varies from zero to the values much larger than Δ. In this parameter regime, the behavior of this system is still not clear.

2. Model and formalism

The structure of a SNS junction on topological insulator surface is schematically displayed in Fig. 1(a) and (c). The bulk s-wave superconductor interacts with the surface electrons of TI by the proximity effect, and the superconductivity is induced in the topological surface states [14,16–26]. The interfaces between superconductor (SC) and normal segment are parallel to y direction. The normal segment is located between $x = -L/2$ and $x = L/2$. With this setup, in the Nambu notation $\Psi = ((\psi_\uparrow, \psi_\downarrow), (\psi_\downarrow^\dagger, -\psi_\uparrow^\dagger))^T$, where $\psi_{\uparrow(\downarrow)}$ is the electron field operator with spin up $\uparrow$ (down $\downarrow$), the SNS junction can be described by the Bogoliubov–de Gennes equation [14,25,26],

$$\begin{pmatrix} \upsilon_F \hat{\sigma} \cdot \hat{p} - \mu(r) & \hat{\Delta} \\ \hat{\Delta}^* & \mu(r) - \upsilon_F \hat{\sigma} \cdot \hat{p} \end{pmatrix} \psi(x, y) = \varepsilon \psi(x, y), \qquad (1)$$

with Pauli matrices $\hat{\sigma} = (\hat{\sigma}_x, \hat{\sigma}_y, \hat{\sigma}_z)$, the in-plane electron momentum $\hat{p} = (\hat{p}_x, \hat{p}_y, 0)$, the Fermi velocity υ_F and the chemical potential $\mu(r)$ which is measured with respect to the Dirac point. $\psi(x, y)$ is the wave function, and ε is the excitation energy. The piecewise chemical potential $\mu(r)$ is μ_N in the middle normal region, and μ_S in left and right superconducting regions. μ_N and μ_S could be tuned independently [16,34,35]. $\hat{\Delta} = \Delta e^{i\varphi}$ is the superconducting pair potential, and Δ is the superconducting energy-gap. The phase φ of superconductor is ϕ_1 and ϕ_2 in the left and right superconducting regions, respectively. Here we presume the distance L between the two interfaces shorter than the superconducting coherence length $\xi = \hbar\upsilon_F/\Delta$ [33,36].

Solving Eq. (1), under the condition of $\mu_S \gg \Delta$, we obtain the wave function in the left superconducting region as

$$\psi_{ls} = \left(a\Psi_a e^{ik_{x0}x} + b\Psi_b e^{-ik_{x0}x}\right) e^{Kx + ik_y y}, \qquad (2)$$

where $\Psi_a = (e^{i(\phi_1 - \gamma - \alpha)}, e^{i(\phi_1 - \alpha)}, e^{-i\gamma}, 1)^T$, $\Psi_b = (-e^{i(\phi_1 + \gamma + \alpha)}, e^{i(\phi_1 + \alpha)}, -e^{i\gamma}, 1)^T$, $k_{x0} = \sqrt{(\mu_S/\hbar\upsilon_F)^2 - k_y^2}$, $K = \frac{\mu_S \Delta \sin\alpha}{\hbar^2 \upsilon_F^2 k_{x0}}$, $\alpha = \arccos(\varepsilon/\Delta)$ for $\varepsilon < \Delta$, the incident angle of the quasiparticles $\gamma = \arcsin(\hbar\upsilon_F k_y/\mu_S)$, a and b are the amplitudes of coherent superpositions of electron and hole excitations, which decay exponentially as $x \to -\infty$.

The wave function in the middle normal region ψ_n depends on μ_N, where $\mu_N \geq 0$ is assumed. If $0 \leq \varepsilon < \mu_N$, we have

$$\psi_n = \left[c\Psi_c e^{ik_x x} + d\Psi_d e^{-ik_x x} + f\Psi_f e^{ik_{x1}x} + g\Psi_g e^{-ik_{x1}x}\right] e^{ik_y y}, \qquad (3)$$

where $\Psi_c = (e^{-i\theta}, 1, 0, 0)^T$, $\Psi_d = (-e^{i\theta}, 1, 0, 0)^T$, $\Psi_f = (0, 0, e^{-i\theta'}, 1)^T$, $\Psi_g = (0, 0, -e^{i\theta'}, 1)^T$, $\theta = \arcsin\frac{\hbar\upsilon_F k_y}{\mu_N + \varepsilon}$ and $k_x = \frac{\mu_N + \varepsilon}{\hbar\upsilon_F} \times \cos\theta$ for electrons in the case of $|\frac{\hbar\upsilon_F k_y}{\mu_N + \varepsilon}| \leq 1$. When $|\frac{\hbar\upsilon_F k_y}{\mu_N + \varepsilon}| > 1$, $\theta = \mathrm{sign}(\gamma)(\frac{\pi}{2} - i\,\mathrm{arccosh}|\frac{\hbar\upsilon_F k_y}{\mu_N + \varepsilon}|)$, and $k_x = i\frac{\mu_N + \varepsilon}{\hbar\upsilon_F}\sinh(\mathrm{arccosh}|\frac{\hbar\upsilon_F k_y}{\mu_N + \varepsilon}|)$. $\theta' = \arcsin\frac{\hbar\upsilon_F k_y}{\mu_N - \varepsilon}$, and $k_{x1} = \frac{\mu_N - \varepsilon}{\hbar\upsilon_F}\cos\theta'$ for holes in the case of $|\frac{\hbar\upsilon_F k_y}{\mu_N - \varepsilon}| \leq 1$. When $|\frac{\hbar\upsilon_F k_y}{\mu_N - \varepsilon}| > 1$, $\theta = \mathrm{sign}(\gamma)(\frac{\pi}{2} - i\,\mathrm{arccosh}|\frac{\hbar\upsilon_F k_y}{\mu_N - \varepsilon}|)$, and $k_x = i\frac{\mu_N - \varepsilon}{\hbar\upsilon_F}\sinh(\mathrm{arccosh}|\frac{\hbar\upsilon_F k_y}{\mu_N - \varepsilon}|)$. c and d are the amplitudes of the right and left moving electrons, and f and g are the amplitudes of the left and right moving holes. The incident electron is reflected as a hole through retro-reflection (normal Andreev reflection) as presented in Figs. 1(a) and 1(b) [37].

If $\varepsilon = \mu_N \neq 0$ [38,39], we obtain

$$\psi_n = \left[c\Psi_c e^{ik_x x} + d\Psi_d e^{-ik_x x} + f\Lambda_4 e^{-k_y x} + g\Lambda_3 e^{k_y x}\right] e^{ik_y y}, \qquad (4)$$

where $\Lambda_3 = (0, 0, 1, 0)^T$, $\Lambda_4 = (0, 0, 0, 1)^T$, θ, k_x, c and d are defined as above, f and g are the amplitudes of wave functions for the right and left moving holes, which are evanescent wave functions.

If $\varepsilon = \mu_N = 0$ [38,39], the wave function is

$$\psi_n = \left(c\Lambda_2 e^{-k_y x} + d\Lambda_1 e^{k_y x} + f\Lambda_4 e^{-k_y x} + g\Lambda_3 e^{k_y x}\right) e^{ik_y y}, \qquad (5)$$

where $\Lambda_1 = (1, 0, 0, 0)^T$, $\Lambda_2 = (0, 1, 0, 0)^T$, c and d are the amplitudes of the right and left decaying wave of electrons, f and g are the amplitudes of the right and left decaying wave of holes.

If $\varepsilon > \mu_N$, we get

$$\psi_n = \left(c\Psi_c e^{ik_x x} + d\Psi_d e^{-ik_x x} + f\Psi_g^* e^{ik_{x1}x} + g\Psi_f^* e^{-ik_{x1}x}\right) e^{ik_y y}, \qquad (6)$$

where θ (in Ψ_c and Ψ_d), c, and d are defined as above, but θ' (in Ψ_f and Ψ_g) is given by $\theta' = \arcsin\frac{\hbar\upsilon_F k_y}{\varepsilon - \mu_N}$, and $k_{x1} = \frac{\varepsilon - \mu_N}{\hbar\upsilon_F}\cos\theta'$ for holes, when $|\frac{\hbar\upsilon_F k_y}{\varepsilon - \mu_N}| \leq 1$. When $|\frac{\hbar\upsilon_F k_y}{\varepsilon - \mu_N}| > 1$, $\theta' = \mathrm{sign}(\gamma)(\frac{\pi}{2} - i\,\mathrm{arccosh}|\frac{\hbar\upsilon_F k_y}{\varepsilon - \mu_N}|)$, and $k_{x1} = i\frac{\varepsilon - \mu_N}{\hbar\upsilon_F}\sinh(\mathrm{arccosh}|\frac{\hbar\upsilon_F k_y}{\varepsilon - \mu_N}|)$. f and g are the amplitudes of the right and left moving holes. The incident electron is reflected as a hole through the specular reflection as presented in Figs. 1(c) and 1(d) [33].

The wave function in the right superconductor is:

$$\psi_{rs} = \left(h\Psi_h e^{-ik_{x0}x} + j\Psi_j e^{ik_{x0}x}\right) e^{-Kx + ik_y y}, \qquad (7)$$